České vysoké učení technické v Praze
Fakulta jaderná a fyzikálně inženýrská

Czech Technical University in Prague
Faculty of Nuclear Sciences and Physical Engineering

Habilitační přednáška

Partonová saturace při vysokoenergetických srážkách

Parton saturation in high energy collisions

Praha, 2021

Ing. Jan Čepila, Ph.D.

Souhrn

Následující text shrnuje poznatky o struktuře protonů a jader v kontextu jevu partonové saturace. Tato práce je formulována pomocí modelu barevného dipolu, kde fyzikální informace je obsažena v tzv. dipolové amplitudě rozptylu. Tento objekt můžeme získat jako řešení integro-diferenciální rovnice s názvem Balitsky-Kovchegovova (BK) rovnice, která je odvozena z formálního poruchového rozvoje Lagrangiánu QCD, nebo pomocí modelu inspirovaného chováním QCD. Řešení plné BK rovnice je velmi komplikované, jak z hlediska fyzikální interpretace tak z hlediska technického. Prvotní zjednodušená řešení předpokládala homogenní nekonečně velký hadronový terč. Avšak v současnosti lze už BK rovnici řešit pro terč konečných rozměrů. Hadronové terče mají kromě konečných rozměrů i konstituenty, které fluktuují v čase. Současné metody řešení BK rovnice neumožňují studovat tyto fluktuace přímo. Proto byl navržen model hadronového terče formulovaný pomocí fluktuujících kapek, reprezentujících oblasti s velkou hustotou gluonových polí. V rámci tohoto modelu byl pozorován důležitý projev saturace - dissociativní účinný průřez jako funkce energie srážky roste až do maxima a následně klesá. Navíc poloha tohoto maxima je v oblasti měření současných a plánovaných urychlovačů. Nakonec je prezentována aplikace modelů na pozorovatelné veličiny v procesech jako hluboce nepružný rozptyl, produkce vektorových mesonů a difraktivní hluboce nepružný rozptyl.

Summary

The following text summarizes understanding of the structure of the proton and nuclei in the context of parton saturation. This work has been developed within the color-dipole approach, where the physics is encoded in the dipole scattering amplitude. This object can be obtained by solving an integro-differential equation, the Balitsky-Kovchegov (BK) equation, obtained from a formal perturbative expansion of QCD, or by proposing a QCD-inspired model. The solution of the full BK equation is complicated, both from the point of view of physics and technically. The first solutions, in order to simplify the problem, assumed a homogeneous and infinite hadronic target. However, at current stage of knowledge, the BK equation can be solved for a finite target. The hadronic targets, in addition to have a finite size, are composed of fields that fluctuate event-by-event. The current state of the art in the solution of the BK equation does not allow to study these fluctuations directly. Therefore, a model of hadron targets is proposed made of fluctuating hot spots, representing regions with a high density of gluons fields. With this model, a new and striking signature for saturation was discovered: the dissociative cross section reaches a maximum, as a function of energy, and then decreases. Furthermore, this maximum is within the reach of current and planned accelerators. Finally, the application to observables from processes of the deep-inelastic scattering, vector meson production and diffractive deep-inelastic scattering is presented.

Klíčová slova:
kvantová chromodynamika, partonová saturace, Balitsky-Kovchegovova rovnice, hluboce nepružný rozptyl, produkce vektorových mesonů¨

Keywords:
quantum chromodynamics, parton saturation, Balitsky-Kovchegov equation, deep-inelastic scattering, vector meson production

Contents

1 Introduction

According to the current state of knowledge, one can recognize four fundamental forces in the Universe: gravitational, electromagnetic, weak and strong. The strong force acts between color charged objects and it is responsible for the existence of hadrons, e.g. protons and neutrons and of nuclei. However, the mechanism behind the strong force is not yet fully understood.

The most successful theory that describes the strong force is the Standard Model, via the part called the quantum chromodynamics (QCD). QCD is a relativistic quantum field theory that describe the structure of hadrons in terms of quark and gluon fields. Gluons are the force carriers of the theory. Quarks are the building blocks that constitute matter. Due to the non-abelian nature of this theory, it is possible for a gluon to be splitted into two gluons and also it is possible that two gluons recombine into a single gluon.

The dynamics of QCD is defined by its Lagrangian, which is fully known. However, the fact that the Lagrangian of the interaction is known does not mean that the transformation of the Lagrangian to the equations of motion and their solution for relevant fields can be done easily. Owing to the complexity of the theory, no exact solutions of the full QCD have been found so far. Meanwhile, we have to resort to approximations that simplify the solution. The commonly used approximating method is to use the perturbative series in powers of the strong coupling constant known from quantum mechanics.

Using the perturbative method in QCD leads to the formulation of the Feynman rules for different parts of the scattering flow diagram in analogy to quantum electrodynamics. These rules can be used to formulate the scattering amplitude of the process and by squaring the amplitude also the cross section of the process. The use of perturbative QCD was so far very successful in the description of different observables. However, the omitting of non-perturbative effects led to disagreement of predictions with measured data in certain situations and so there were attempts to solve the disagreement by including phenomena that are able to describe the observed discrepancy. One of the problems, where non-perturbative effects play a crucial role is the description of the structure of the proton in terms of quark and gluon fields.

2 Parton saturation via the Balitsky-Kovchegov equation

Very precise measurements of inclusive data from deep-inelastic scattering at HERA [1] have shown that the proton structure function $F_2(x, Q^2)$ is dominated by gluons at low Bjorken variable x. The number of gluons rises towards larger values of the virtuality, $\ln Q^2$, of the photon at fixed x, but their size gets smaller. This behavior is known to be the result of the Dokshitzer-Gribov-Lipatov-Altarelli-Parisi (DGLAP) evolution equations. On the other hand, the number of gluons inside a proton rises steeply towards small values of the Bjorken variable x with fixed values of the virtuality Q^2, which corresponds to the high-energy limit of QCD.

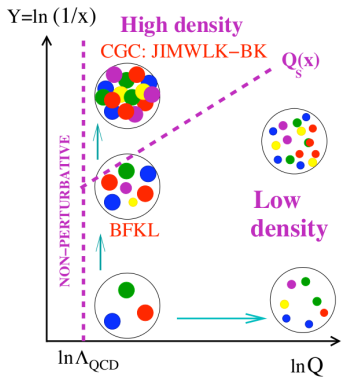

Figure 1: Evolution of parton density in different kinematical regions. Figure taken from [2]

This rise corresponds to the growth of the gluon distribution function for decreasing x at a fixed scale and it was understood to be due to a gluon-branching process. This branching process was encoded in an integro-differential equation describing the evolution of the gluon distribution function in the hadron phase space called the Balitsky-Fadin-Kuraev-Lipatov (BFKL) evolution equation, schematically written as $\partial_y N = K \otimes N$, where K is the kernel of the equation and N is the probability of interaction related to the gluon distribution. In contrast to the DGLAP case, the evolved gluons do not have smaller sizes, but

they have smaller Bjorken x, due to momentum conservation in the branching vertex. While the transverse phase space of the proton is not filled (dilute regime) and the gluon wave functions do not overlap, the evolution is linear. The unitarity of the cross section encoded in the Froissard bound [3] implies that the growth of the gluon density should be tamed at some point. This phenomenon is known as parton (quark and gluon) saturation. A first model of gluon saturation in QCD was presented in the seminal work [4], where a nonlinear term was added to the BFKL evolution equation of the gluon distribution, schematically $\partial_y N = K \otimes (N - N^2)$. As a result, after the branching processes fills the transverse phase space of the proton (dense regime) and the evolution crosses the saturation scale, the wave functions of individual gluons start to overlap and recombination processes may occur. Therefore, the number of gluons is given as the result of a dynamical balance between emission and recombination processes.

A framework to study saturation phenomena is the Color Glass Condensate (CGC); an effective theory, which describes the high-energy limit of QCD [5]. The CGC in the nonlinear regime and in the limit of large number of colors proposes a non-linear evolution equation for the scattering amplitude N of a dipole off the CGC matter. It was independently derived by Balitsky [6] and by Kovchegov [7] within the color dipole model. This equation is called the Balitsky–Kovchegov (BK) equation.

The BK equation is a four dimensional integro-differential equation with an infrared divergent kernel. The solution of the BK equation depends in principle on two 2-dimensional vectors: an usual choice for these vectors is to take the impact parameter of the dipole with respect to the target $\vec{b}$ and the size of the dipole $\vec{r}$.

Up to now, there is no analytic solution for the BK equation, it has to be solved numerically. The numerical solution requires a lot of resources. Partially because of this, N was assumed to take the form

$$N(\vec{r}, \vec{b}) = \sigma_0 N(|\vec{r}|). \tag{1}$$

That is, it was assumed that the target was homogeneous, isotropic and infinitely large.

The solutions of the BK equation assuming dependence on only one variable $|\vec{r}|$ have been used to describe a variety of HERA data:

inclusive, diffractive and exclusive production of vector mesons. The assumption of Eq. (1) was reasonable in the sense that all other degrees of freedom were integrated out and replaced by one constant which in a sense correspond to the realization of an inclusive measurement.

One of the main problems of this version of the BK equation (rcBK) is that the kernel of this integro-differential equation was derived using leading-logarithmic approximation and thus it neglects higher order diagrams. Recently, attempts to include more diagrams into the kernel was done in [8] leading to the so-called collinearly improved Balitsky-Kovchegov equation (ciBK). Results of the solution of ciBK without an impact-parameter dependence were successfully used to describe data from HERA for inclusive deep-inelastic scattering (DIS) [8].

The first successful attempt to find a solution of the equation with an explicit impact-parameter dependence was done in collaboration with my colleagues in [9, 10].

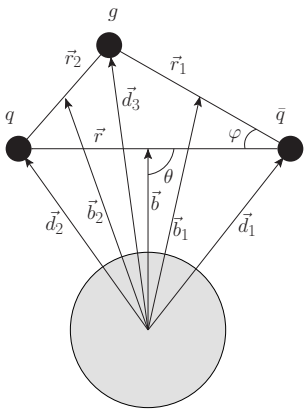

Figure 2: Schematics of the emission of the daughter dipole from the parent dipole and its interaction with a target

The BK equation describes the evolution in rapidity $y = \ln(x_0/x)$ corresponding to Bjorken x, of the scattering amplitude $N(\vec{r}, \vec{b}, y)$ for the scattering of a color dipole of transverse size $\vec{r} = \vec{d_1} - \vec{d_2}$ with a target at a distance $\vec{b} = (\vec{d_1} + \vec{d_2})/2$, see Fig. 2. During the evolution the "parent" dipole may split into two "daughter" dipoles with the sizes $\vec{r_1} = \vec{d_1} - \vec{d_3}$ and $\vec{r_2} = \vec{d_2} - \vec{d_3}$ or, due to the nonlinear term, two

"daughter" dipoles can recombine into one dipole. The general form of the equation was given in [6, 7]

$$\frac{\partial N(\vec{r},\vec{b},y)}{\partial y} = \int d\vec{r}_1 K(\vec{r},\vec{r}_1,\vec{r}_2)\big(N(\vec{r}_1,\vec{b}_1,y)+N(\vec{r}_2,\vec{b}_2,y) - N(\vec{r},\vec{b},y) - N(\vec{r}_1,\vec{b}_1,y)N(\vec{r}_2,\vec{b}_2,y)\big). \quad (2)$$

2.1 Deep-inelastic scattering

One of the most studied processes in the last decades is the deep-inelastic scattering of an electron off a proton target. It is mostly due to the rich and precise collection of data measured by the HERA experiments H1 and ZEUS (see e.g. [1]).

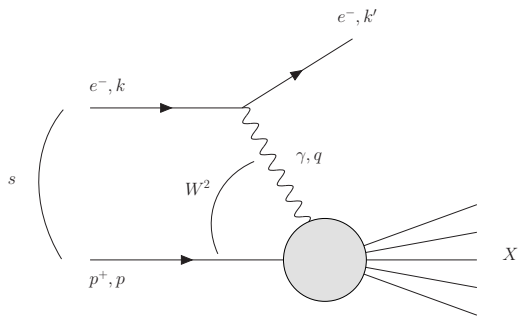

Figure 3: Schematics of the deep-inelastic process.

The incident electron with four-momentum k emits a virtual photon with four-momentum $q = (k - k')$ and continues outward with four-momentum k'. The photon interacts with the target proton with four-momentum p producing a system of hadrons X. The scale of the process is given by the square of the four-momentum of the exchanged photon $Q^2 = -q^2$ and the square of total collision energy in the center-of-mass (cms) frame is $s = (k + p)^2$. The cms energy of the photon-proton system, which is available for the production of final state hadrons, is $W^2 = (q + p)^2$.

In a quantum field theory treatment of the DIS process, one can express the cross section via two form factors F_2 and F_1 (or usually $F_L = F_2 - 2xF_1$) and these form factors incorporate the structure of

the proton. In the Feynman parton model, this structure can be build from the contributions of individual partons (quarks and gluons) that are present in the proton during the interaction and that carry longitudinal momenta xp, where $x = Q^2/2pq = Q^2/(Q^2 + W^2)$ is the fraction of momenta of proton carried by the parton in the infinite momentum frame. Therefore, if we want to study the evolution of the parton probabilities in the proton we have to extract F_2 and F_L from experimental data and compare them to a model that allows us to calculate them.

At high energies it is advantageous to form such model using the color dipole approach [11]. It treats the interaction in the rest frame of

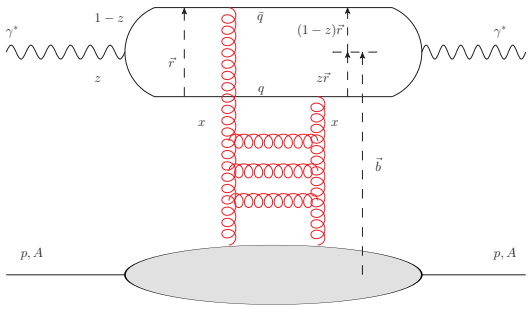

Figure 4: Interaction scheme of the deep-inelastic scattering in color dipole approach with $q\bar{q}$ Fock state.

the proton, where the incoming photon is taken as an infinite ladder of Fock states built from partons that have the quantum numbers of the original photon and carry no net color. During the interaction, one of the Fock states exchanges a colorless object with the quantum numbers of the vacuum, called the Pomeron, with the target proton. Using the QCD degrees of freedom, the simplest approximation of the Pomeron is a pair of gluons with opposite color and anti-color. Taking the most probable Fock state being a $q\bar{q}$ pair one can depict the process as in Fig. 4

The proton structure functions $F_2(x, Q^2)$ and $F_L(x, Q^2)$ are related to the total cross section $\sigma^{\gamma^* p}$ for the scattering of a virtual photon γ^*

off a proton as [11, 12]

$$
\begin{aligned}
F_2(x,Q^2) &= \frac{Q^2}{4\pi^2\alpha_{em}}(\sigma_T^{\gamma^* p}(x,Q^2)+\sigma_L^{\gamma^* p}(x,Q^2)) \\
F_L(x,Q^2) &= \frac{Q^2}{4\pi^2\alpha_{em}}\sigma_L^{\gamma^* p}(x,Q^2),
\end{aligned} \tag{3}
$$

where x is the Bjorken x, Q^2 is the scale of the process, α_{em} is the fine-structure constant, $\sigma_{T,L}^{\gamma^* p}(x,Q^2)$ are the transversal and longitudinal cross sections of the scattering of a transversally or longitudinally polarized virtual photon with a target proton, respectively. They can be calculated in the light-cone color dipole model [11–13] as

$$
\sigma_{T,L}^{\gamma^* p}(x,Q^2) = \int \mathrm{d}\vec{r} \int_0^1 \mathrm{d}z |\psi_{\gamma^*\to q\bar{q}}^{T,L}(\vec{r},z,Q^2)|^2 \sigma_{q\bar{q}}(\vec{r},\tilde{x}), \tag{4}
$$

where $\sigma_{q\bar{q}}(\vec{r},x)$ is the cross section for the interaction of a quark-antiquark dipole with the target proton, $\psi_{\gamma^*\to q\bar{q}}^{T,L}(\vec{r},z,Q^2)$ are wave functions (probability amplitudes) of a situation where a photon splits into a quark-antiquark pair, $\vec{r}$ is the transverse dipole size, $\vec{b}$ is the impact parameter of the dipole and z is the fraction of the photon momentum carried by one of the quarks from the dipole and $\tilde{x}$ is a Bjorken x of the exchanged Pomeron.

We have successfully calculated the results for DIS structure functions using the impact parameter independent BK evolution equation, see [14]. In the papers [9] and [10] we have extended our model to include the solution of the explicitly impact-parameter dependent BK equation and we have published predictions using this model in kinematic regions for the new facilities, the EIC and the LHeC. So, without any additional parameters our model for the impact parameter dependent BK equation can be used to describe data, see Fig. 5. Both our models describe data for inclusive DIS very well due to the fact that the dipole scattering amplitude enters the cross section formula already integrated over the impact parameter, and so, the difference between both models can be absorbed in the parameters of the impact-parameter independent model.

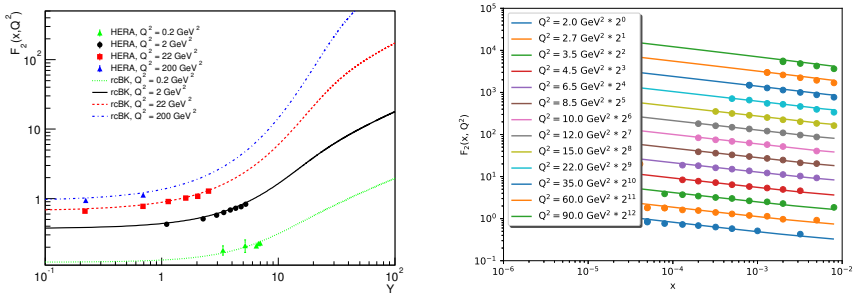

Figure 5: Structure function calculated using the impact parameter independent rcBK (left) and using the impact parameter dependent BK equation (right) compared to HERA data. Both models describe data well in a broad range of scales Q^2.

2.2 Production of vector mesons

The production of vector mesons can be viewed as follows. Consider a photon with four-momenta q emitted from the electron or hadron with four-momenta k. The scale of the photon is $Q^2 = -q^2$. Either Q^2 is very small ~ 0 (photoproduction) or Q^2 is greater than 0 (electroproduction). This photon interacts diffractively with the incoming proton with four-momenta p while a vector meson is produced with four-momenta p^V and the proton is either left intact (exclusive production) or is dissociated into a diffractive hadronic system (dissociative production) with four-momenta x.

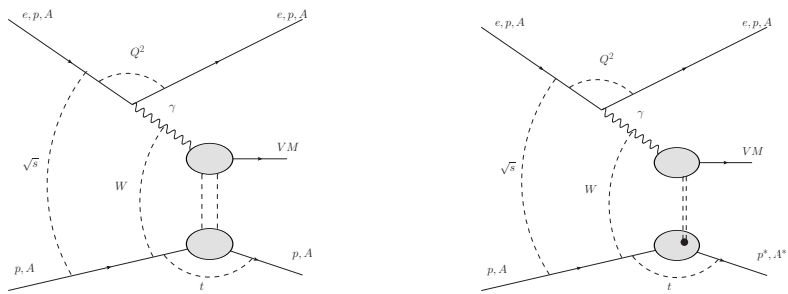

Figure 6: Kinematics of exclusive and dissociative vector meson production

The square of the total energy available for the production of the final state in the cms frame is W^2 and it is related to the square of the total collision energy $s = W^2 + Q^2$. Another kinematic quantity that defines the process is the square of the four-momenta transfer in the proton vertex $t = -Q^2 - (p_T^V)^2$, where p_T^V is the transverse momentum of the outgoing vector meson. In particular, for photoproduction $Q^2 = 0$ we can write $\sqrt{-t} = p_T^V =: \Delta$. The last kinematic variable that is usually defined is the Bjorken x as

$$x = \frac{M_V^2 + Q^2}{W^2 + Q^2} = \frac{M_V}{\sqrt{s}} \exp(-y), \tag{5}$$

where M_V and y are the mass and the rapidity of the vector meson.

The production of a vector meson in the color dipole approach can be calculated in analogy to the DIS case. The amplitude for the production of a vector meson V is given by [15]

$$\mathcal{A}_{T,L}^{\gamma^* p \to Vp} = i \int \mathrm{d}^2 r \int_0^1 \frac{\mathrm{d}z}{4\pi} \int \mathrm{d}^2 b \, \Psi_V^* \Psi_{\gamma^*} \Big|_{T,L} e^{-i(\vec{b}-(1-z)\vec{r})\Delta} \frac{\mathrm{d}\sigma_{q\bar{q}}}{\mathrm{d}^2 b} \tag{6}$$

where $\Psi_V^* \Psi_{\gamma^*}|_{T,L}$ is the overlap of a virtual photon and the vector meson wave function, $\Delta = \sqrt{-t}$ denotes the transverse momentum lost by the proton, $\vec{r}$ is the transverse dipole size, $\vec{b}$ is the impact parameter of the dipole and z is the part of photon momenta carried by one of the quarks from the dipole. The momentum transfer Δ Fourier conjugates to the transverse distance from the center of the proton to one of quarks in the dipole $\vec{b} + (1-z)\vec{r}$. The diffractive differential and total cross section can be written as

$$\frac{\mathrm{d}\sigma_{T,L}^{\gamma^* p \to Vp}}{\mathrm{d}|t|} = \frac{1}{16\pi} \left| \mathcal{A}_{T,L}^{\gamma^* p \to Vp} \right|^2 \qquad \sigma_{T,L}^{\gamma^* p \to Vp} = \int_{t_{min}}^{t_{max}} \frac{\mathrm{d}\sigma_{T,L}^{\gamma^* p \to Vp}}{\mathrm{d}|t|}. \tag{7}$$

The derivation of the previous formulas relies on the assumption that the S-matrix is purely real and so the amplitude $\mathcal{A}$ is purely imaginary. The real part of the amplitude can be accounted for by multiplying the differential cross section by a factor $1 + \beta_{T,L}^2$ as in [16]. Finally, one has to incorporate the fact, that gluons attached to quarks in the $q\bar{q}$ dipole carry different light-front momenta fractions x and x' of the

proton: the skewness effect [17]. It is taken into account by multiplying the cross sections formula with a factor $R_g^2(\lambda_{T,L})$.

We have successfully calculated the results for exclusive vector meson production using the impact parameter dependent BK evolution equation in the paper [10] and we have published predictions using this model in kinematic regions for the new facilities, the EIC and the LHeC. The main results of the paper are shown at Fig. 7, where the $|t|$-distribution for the J/Ψ meson is shown compared to data form HERA.

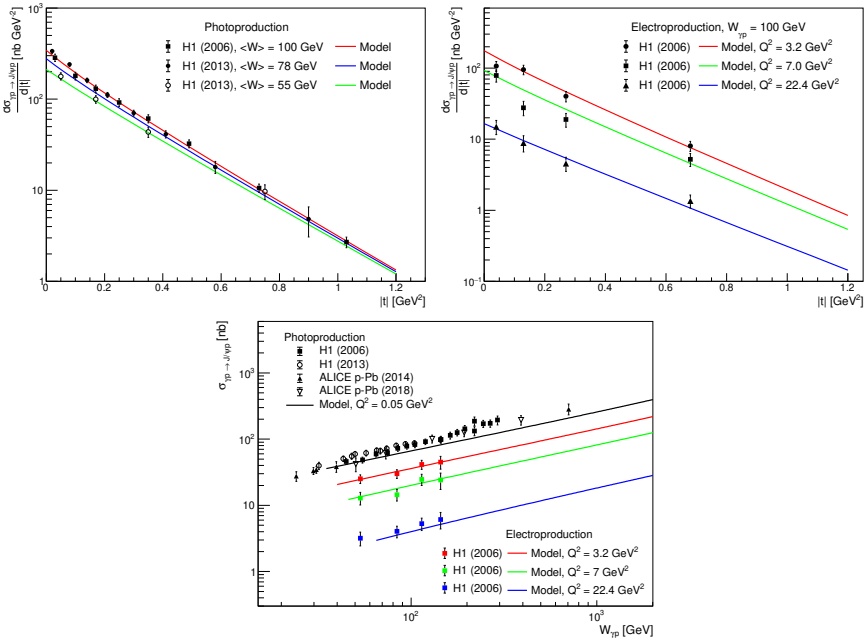

Figure 7: Comparison of the predictions of the model with HERA data from H1 for the $|t|$ dependence of the exclusive photoproduction (left) and electroproduction (right) cross sections of the J/Ψ meson and the W dependence of the total cross section (bottom).

Moreover, there are no additional parameters used and the scattering amplitude is of the same form as was used to calculate DIS while it describes available data from H1 for the $|t|$-distribution of J/Ψ photo and electroproduction and also data for the total cross section from H1 and also form ALICE, see fig 7.

2.3 Diffractive deep-inelastic scattering

Diffractive deep-inelastic scattering is a process where an electron scatters off the hadron leading to an electron + hadron + diffractive system of hadrons denoted as X, where the hadron in the final state carries most of the beam momenta. The scattering can be seen as follows. Consider an electron with four-momentum k, that emits a photon with four-momentum q and goes away with the four-momentum k'. The produced photon with scale $Q^2 = -q^2$ interacts strongly with the incoming hadron with four-momentum p while the target hadron is not dissolved and with a gap in rapidity the hadronic spectrum X with the mass M_X is produced.

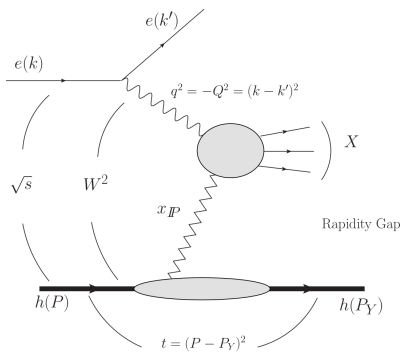

Figure 8: Kinematics of the diffractive deep-inelastic process.

We can define $W^2 = (q+p)^2$ as the center-of-mass energy of the photon-hadron system, $Q^2 = -(k-k')^2$ is the scale of the incoming photon, $s = (k+p)^2 = W^2 + Q^2$ as the cms energy of the collision, $x_{\mathbb{P}} = (Q^2 + M_X^2)/s$ is the fractional longitudinal momentum loss of the hadron and $\beta = Q^2/(M_X^2 + Q^2)$. Using these kinematic variables one can define Bjorken x as $x_{Bj} = \beta x_{\mathbb{P}} = Q^2/s$. The differential cross section for diffractive DIS can be expressed as (see e.g. [18])

$$\frac{d\sigma^{eh\to eXh}}{d\beta dQ^2 dx_{\mathbb{P}}} = \frac{4\pi\alpha^2}{\beta Q^4}\left[1 - y + \frac{y^2}{2}\right]\Big(F_2^{D(3)}(x_{\mathbb{P}}, \beta, Q^2) - \frac{y^2}{1+(1-y)^2}F_L^{D(3)}(x_{\mathbb{P}}, \beta, Q^2)\Big), \tag{8}$$

where y is the fractional energy loss of the electron in the hadron rest frame and $F_2^{D(3)}$ and $F_L^{D(3)}$ are diffractive structure functions. If we restrict ourselves to the two simplest states $q\bar{q}$ and $q\bar{q}g$, we can write in the color dipole approach

$$F_2^{D(3)} = F_{T,q\bar{q}}^D + F_{L,q\bar{q}}^D + F_{T,q\bar{q}q}^D (+F_{L,q\bar{q}q}^D),$$

where T, L denote the transverse and longitudinal degrees of freedom of the photon. For the $q\bar{q}g$ contribution, only the transverse polarization is usually considered, since the longitudinal counterpart has no leading logarithm in Q^2. Individual contributions derived in the color dipole formalism are in e.g. [19]

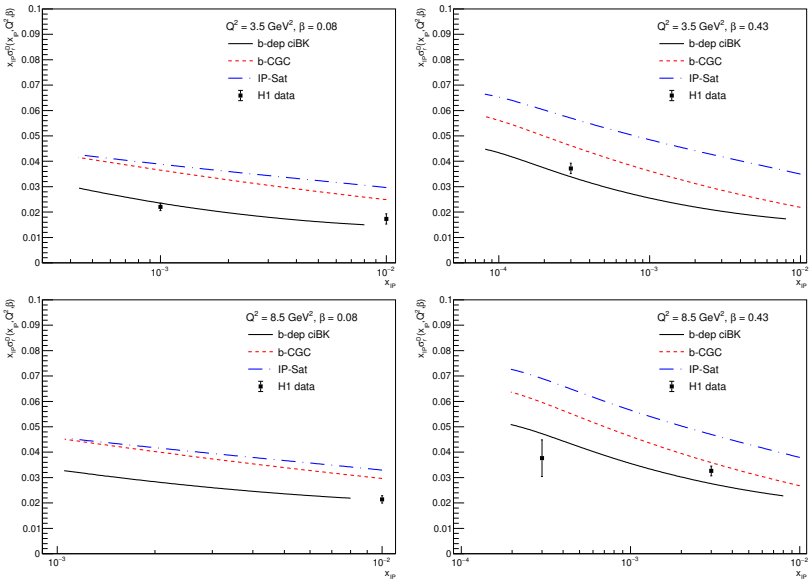

Figure 9: Predictions for the $x_{\mathbb{P}}$-dependence of the reduced diffractive cross section at different combinations of the photon virtuality and β, considering the b-CGC, IP-Sat, and b-dep ciBK models for the dipole-proton scattering amplitude. Data from H1 are presented for comparison.

In [20] we have presented, for the first time, predictions for the diffractive structure functions and reduced diffractive cross sections derived using the solution of the impact-parameter dependent Balitsky-Kovchegov equation for the dipole-target scattering amplitude, see Fig.

9. Note, that the solution of the BK equation can be used without any additional parameter in the same form as was used for the calculation of DIS and vector meson observables. Our results for collisions off a proton target indicate that the BK equation describes the existing data well and implies a smaller normalization for the reduced cross section in comparison to phenomenological models based on the CGC physics.

3 The hot-spot model

Perturbative QCD predicts that the gluon density in hadrons grows with energy, or equivalently with decreasing Bjorken x, up to a point where nonlinear effects manifest to slow down this growth, a phenomenon known as gluon saturation. Exclusive and dissociative vector meson photoproduction, see Fig 6, is sensitive to the distribution of gluons in the impact parameter plane, through the dependence of the cross section on t, the square of the momentum transfer at the target vertex. The kinematics of the process are summarized in Sec. 2.2. While the exclusive process, where the target hadron remains intact, is easy to calculate within the color dipole approach, see Sec. 2.2, the dissociative process, where the target hadron is dissolved, is harder to calculate directly and one has to rely on a more general procedure. In a Good-Walker formalism [21] exclusive diffractive processes are proportional to the average over the different configurations of the target, while dissociative processes, where the target gets excited and produces many particles, measure the variance over the configurations [22].

Diagrams for the exclusive and dissociative production of vector mesons are shown in Fig. 6, where the photon source is a proton or a Pb ion. In the dipole color model [11, 12], the exclusive and dissociative production of vector mesons proceeds as follows. A photon with virtuality Q^2 fluctuates into a coherent quark-antiquark pair with the transverse distance $\vec{r}$, then this pair interacts with the target proton at an impact parameter $\vec{b}$ with the color dipole cross section $\sigma_{\rm dip}$ at total energy W and forms a vector meson with mass M_V and Bjorken $x = (M_V^2 + Q^2)/(W^2 + Q^2)$. In the exclusive case, the target proton remains intact while in the dissociative case the proton is resolved. In this approach the amplitude is written in Sec. 2.2.

The physics of the interaction is encoded in the dipole-target cross

section, which is related, via the optical theorem, to the imaginary part of the forward dipole-target amplitude $N(x, \vec{r}, \vec{b})$ as

$$\frac{d\sigma_{\rm dp}}{d\vec{b}} = 2N(x, \vec{r}, \vec{b}) = \sigma_0 N(x, r) T_p(\vec{b}). \tag{9}$$

In order to use the impact parameter integrated dipole amplitude a factorized form for the dipole cross section (see [23]) is used, where $\sigma_0 \equiv 4\pi B_p$ is a constant that provides the normalization and $T_p(\vec{b})$ describes the proton profile in the impact parameter plane and the form of $N(x, r)$ given by e.g. the GBW model [24]

$$N^{\rm GBW}(x, r) = \left(1 - e^{-\frac{r^2 Q_0^2}{4}(x_0/x)^\lambda}\right) \qquad Q_0^2 = 1 \text{ GeV}^2, \tag{10}$$

where λ and x_0 are free parameters.

The proton is a quantum object, so its structure fluctuates from interaction to interaction. In this model fluctuations are included in the proton profile $T_p(\vec{b})$. Following [25] the proton profile is defined as the sum of $N_{hs}(x)$ regions of high-gluon density, so called hot spots, each of them having a Gaussian distribution with fixed size $B_{hs} = 0.8 \text{ GeV}^{-2}$ that are placed at positions $\vec{b}_i$ generated from a 2-D Gaussian distribution centered at $(0, 0)$ and having the width $B_p = 4.7 \text{ GeV}^{-2}$, see Fig. 10. The final formula reads [25, 26]

$$T_p(\vec{b}) = \frac{1}{N_{hs}(x)} \sum_{i=1}^{N_{hs}(x)} T_{hs}(\vec{b} - \vec{b}_i) \qquad T_{hs}(b) = \frac{1}{2\pi B_{hs}} e^{-\frac{b^2}{2B_{hs}}}, \tag{11}$$

where the number of hot spots $N_{hs}(x)$ is an unknown functional parameter of the model. We took $N_{hs}(x)$ to be the random number from the zero-truncated Poisson distribution, where its mean value comes from a formula very loosely motivated by parton distribution parametrizations [25, 26]

$$\langle N_{hs}(x) \rangle = 0.011 x^{-0.58}(1 + 300\sqrt{x}), \tag{12}$$

where we presume that the number of hot spots will rise with decreasing Bjorken x. The new ingredient in this model is that it introduces an indirect energy dependence of the proton profile $T_p(\vec{b})$ by making the number of hot spots grow with decreasing x (see [27]). This implements

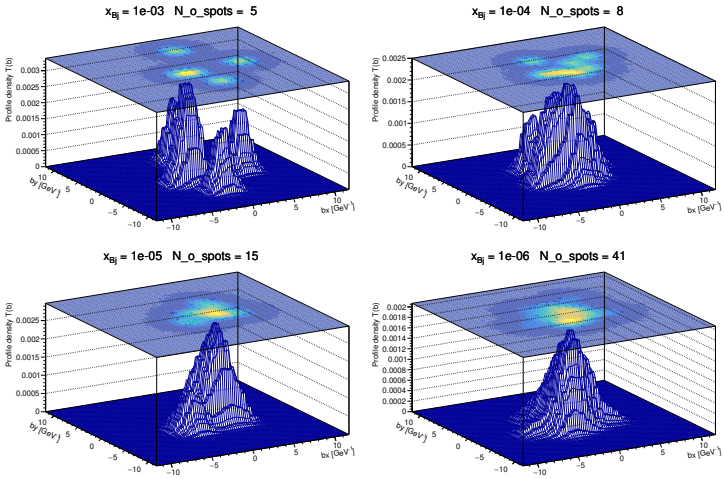

Figure 10: The figure shows examples of profiles generated from hot spots at different Bjorken-x. Since the formula for scattering amplitude no longer depends on the magnitude of the impact parameter, we have to use 2-D distribution in contrast to standard profile functions. For details see [25].

the hypothesis that, at a given fixed scale, as energy increases, the number of gluons available for the interaction increases.

Using the above mentioned amplitude in accordance to the Good-Walker approach, the cross sections are an average over the configurations

$$\frac{d\sigma(\gamma p \to Vp)}{dt} = \frac{R_g^2}{16\pi} \left| \left\langle A^j(x, Q^2, \vec{\Delta}) \right\rangle \right|^2 , \tag{13}$$

for the exclusive process, and a variance over the configurations

$$\frac{d\sigma(\gamma p \to VY)}{dt} = \frac{R_g^2}{16\pi} \left(\left\langle \left| A^j(x, Q^2, \vec{\Delta}) \right|^2 \right\rangle - \left| \left\langle A^j(x, Q^2, \vec{\Delta}) \right\rangle \right|^2 \right) , \tag{14}$$

for dissociative production, see Sec. 2.2.

The parameters of the model were fixed as follows (see the discussion in [25]. The value of λ is constrained by the data for the energy dependence of exclusive J/Ψ photoproduction from HERA to $\lambda = 0.21$. The parameter B_p is constrained by the t distribution of the same data at $\langle W \rangle = 78$ GeV and set to $B_p = 4.7$ GeV^{-2} and the parameter $\sigma_0 \equiv 4\pi B_p$. The x_0 parameter is strongly correlated to σ_0, so once

B_p is fixed, the normalization of the data yields $x_0 = 0.0002$. The parameter B_{hs} is constrained by the data for the t dependence of the dissociative process from HERA and it is set to $B_{hs} = 0.8$ GeV^{-2}. Note that the parameters are chosen so that they describe simultaneously the energy dependence of H1 measurements of exclusive and dissociative J/Ψ photoproduction.

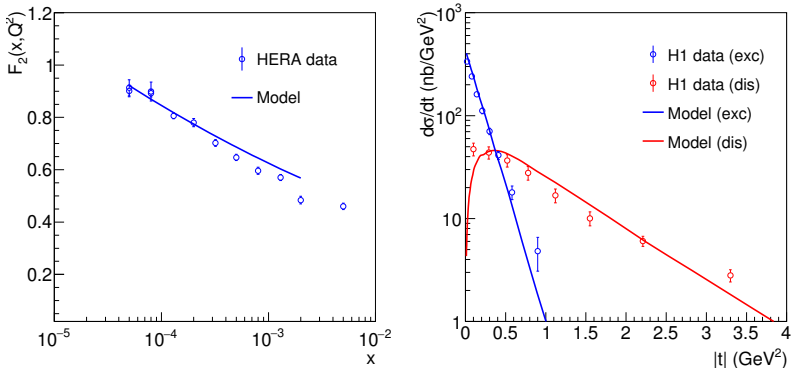

Figure 11: Left: Results for the structure function F_2 calculated using formulas from Sec. 2.1 with the proton transverse profile composed of hot spots. Right: Comparison of the model to data on the $|t|$ distribution of exclusive (blue) and dissociative (red) photoproduction of J/Ψ as measured by H1 at $\langle W \rangle = 78$ GeV.

Although the model is relatively simple and has been developed to describe vector meson photoproduction, it describes well the $F_2(x, Q^2)$ data (see Fig. 11). The comparison with H1 data on the t dependence of J/Ψ photoproduction is shown in the right panel of Fig. 11 for the data at $\langle W \rangle = 78$ GeV. Both the exclusive and the dissociative processes are reasonably well described. The left panel of Fig. 12 shows the energy dependence of the total cross section for the exclusive vector meson production within our model and compares it to data from H1 and ALICE.

Again, the model describes quite well the data. However, when one plots the same energy dependence of the dissociative vector meson production, see the right panel of Fig. 12, one gets not only the correct description of the energy evolution of the dissociative cross section for the available data. We also show that the model predicts that the cross

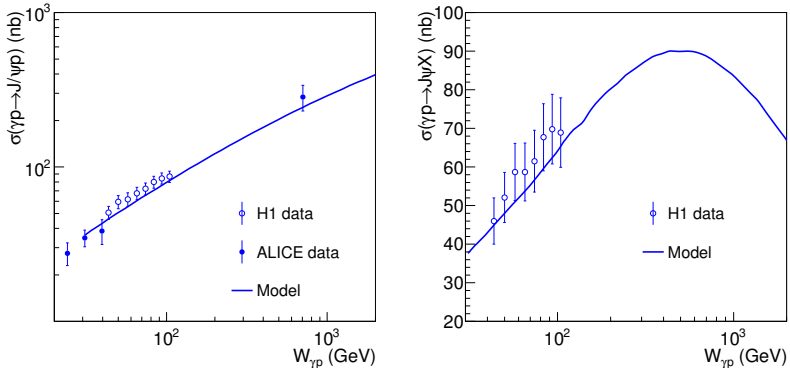

Figure 12: Comparison of the model to data on the W dependence of the cross section for exclusive (left) and dissociative (right) photoproduction of J/Ψ as measured by H1 and ALICE.

section will reach a maximum at $W \approx 500$ GeV and it will then turn around and decrease for higher energies. This decrease of the dissociative J/Ψ photoproduction cross section is a striking feature of our model and it is significantly large to be observed in the W energy range accessible at the LHC. Also, it will be one of the first measurements done at future electron-ion colliders. For the parameters that we have employed in our study, the maximum at $W \approx 500$ GeV is reached when some 10 hot spots are present, indicating a sizeable overlap of hot spots.

The energy dependence of the dissociative cross section has a geometrical property reminiscent of percolation. The interpretation of this behavior is given by the form of the cross section in the Wood-Saxon approach. The dissociative production measures the variance over the different configurations into which the structure of the proton can fluctuate. In our model, this is given by the different geometrical placements of the hot spots in the impact-parameter plane. As the energy W increases, so it does the number of hot spots inside the proton, as shown in Fig. 10. As the hot spots have all the same transversal area, the more hot spots there are, the more the proton area is filled. At some point the number of hot spots is so large that they overlap. At this point, all the possible configurations start to look alike, because all of them start filling all the available area in the proton and overlap in a process reminiscent of percolation. From this energy onwards the

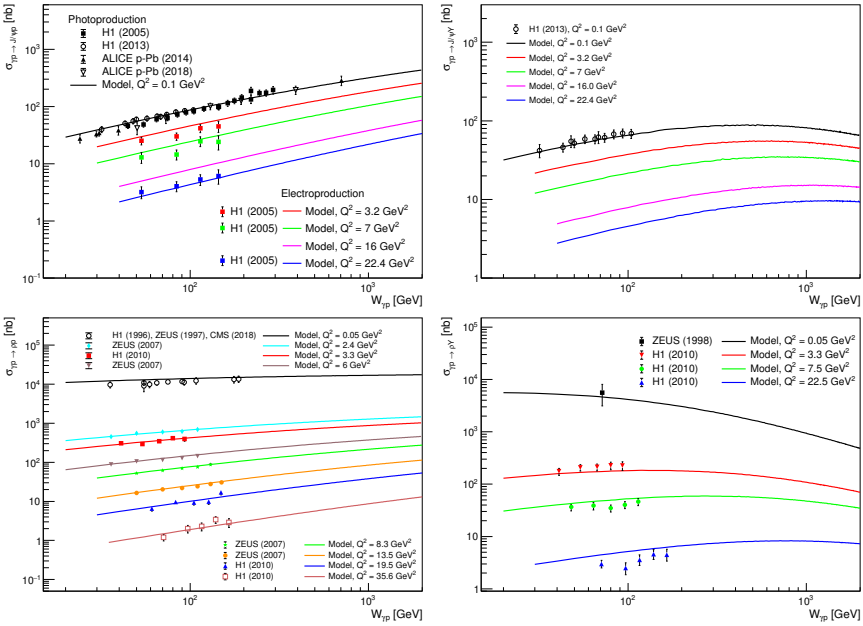

Figure 13: The W dependence of the cross section for exclusive (left) and dissociative (right) production of J/Ψ (upper plots) and ρ (lower plots) as measured by H1, ZEUS, LHCb and CMS.

variance over configurations steeply decreases.

Another striking feature of this discovery is the fact, that it is present for all species and also for electroproduction and the position of maxima shifts to higher energies for an increasing scale of the process and also for an increasing mass of the vector meson, see Fig. 13. The recently published data from the H1 experiment for the dissociative ρ photoproduction from [28] are well in line with our prediction as they show that the cross section decreases with energy. For details, see [29]. Note, that for all of those predictions we have not introduced any additional parameters, and so, all parameters are basically fixed by J/Ψ data measured by HERA experiments.

4 Summary

In [14], I have, together with my colleagues, proposed a novel effective algorithm to solve numerically the rcBK equation at the leading order with running coupling. In [10] and in [30], I have (together with my students and colleagues) successfully modified our algorithm for solving the BK equation to include an explicit impact parameter dependence and we have, for the first time, published in [9] the results for the running coupling leading order kernel and also for the collinearly improved kernel. The inclusion of the impact-parameter dependence in this context allows for a more realistic treatment of the hadronic targets and the combination of the new initial condition with the collinearly improved kernel solve, or suppress strongly, the problems previously encounter when using the rcBK equation, meaning that now the impact parameter dependence can be meaningfully included in studies of pQCD at high energies when comparing to data.

Finally, I have in [20], together with my colleagues, tested our solution of the impact-parameter dependent BK equation on diffractive deep-inelastic scattering off proton and nuclear targets, where we have found good agreement with existing data on proton targets while we have found some very interesting features of our predictions on nuclear targets.

In the series of papers [25–27, 29, 31] we have developed and studied in detail a simple, yet clearly motivated, effective model for vector meson photo and electroproduction off proton and nuclear targets including hot spots randomly sampled into the thickness function of the target hadron that fluctuates event-by-event and that allowed us to calculate the amplitude for exclusive and dissociative vector meson production as a mean value and variance, respectively, over all generated configurations via the Good-Walker approach [21]. This analysis showed a striking feature in the energy dependence of dissociative cross section that does not grow with energy infinitely but rather has a maximum and then it drops to zero reflecting the situation where the growing number of hot spots fills the proton and the variance of such filled proton goes to zero. This finding is partially supported with recent data from HERA experiments and provides a very interesting prediction for one of the fist measurements at future colliders.

References

[1] Abramowicz, H. et al. *Eur. Phys. J.* **C75**(12), 580 (2015).

[2] Marquet, C. *Nucl. Phys. A* **904-905**, 294c–301c (2013).

[3] Froissart, M. *Phys. Rev.* **123**, 1053–1057 Aug (1961).

[4] Gribov, L. V., Levin, E. M., and Ryskin, M. G. *Phys. Rept.* **100**, 1–150 (1983).

[5] McLerran, L. D. and Venugopalan, R. *Phys. Rev.* **D49**, 2233–2241 (1994).

[6] Balitsky, I. *Phys. Rev.* **D75**, 014001 (2007).

[7] Kovchegov, Y. V. and Weigert, H. *Nucl. Phys.* **A784**, 188–226 (2007).

[8] Iancu, E., Madrigal, J. D., Mueller, A. H., Soyez, G., and Triantafyllopoulos, D. N. *Phys. Lett.* **B750**, 643–652 (2015).

[9] Cepila, J., Contreras, J. G., and Matas, M. *Phys. Rev. D* **99**(5), 051502 (2019).

[10] Bendova, D., Cepila, J., Contreras, J. G., and Matas, M. *Phys. Rev.* **D100**(5), 054015 (2019).

[11] Mueller, A. H. *Nucl. Phys. B* **335**, 115–137 (1990).

[12] Nikolaev, N. N. and Zakharov, B. G. *Z. Phys.* **C49**, 607–618 (1991). [,733(1990)].

[13] Nikolaev, N. and Zakharov, B. G. *Z. Phys.* **C53**, 331–346 (1992).

[14] Cepila, J. and Contreras, J. G. *arXiv:hep-ph/1501.06687* (2015).

[15] Kowalski, H., Motyka, L., and Watt, G. *Phys.Rev.* **D74**, 074016 (2006).

[16] Nemchik, J., Nikolaev, N. N., Predazzi, E., and Zakharov, B. *Z.Phys.* **C75**, 71–87 (1997).

[17] Shuvaev, A. G., Golec-Biernat, K. J., Martin, A. D., and Ryskin, M. G. *Phys. Rev. D* **60**, 014015 (1999).

[18] Gonçalves, V., Kugeratski, M., and Navarra, F. *Nucl. Phys. A* **787**, 415–422 (2007).

[19] Kowalski, H., Lappi, T., Marquet, C., and Venugopalan, R. *Phys. Rev. C* **78**, 045201 (2008).

[20] Bendova, D., Cepila, J., Contreras, J. G., Gonçalves, V. P., and Matas, M. *arXiv:hep-ph/2009.14002* 9 (2020).

[21] Good, M. and Walker, W. *Phys. Rev.* **120**, 1857–1860 (1960).

[22] Miettinen, H. I. and Pumplin, J. *Phys. Rev. D* **18**, 1696 (1978).

[23] Marquet, C. *Phys. Rev. D* **76**, 094017 (2007).

[24] Golec-Biernat, K. J. and Wusthoff, M. *Phys.Rev.* **D59**, 014017 (1998).

[25] Cepila, J., Contreras, J. G., and Tapia Takaki, J. D. *Phys. Lett.* **B766**, 186–191 (2017).

[26] Cepila, J., Contreras, J. G., and Krelina, M. *Phys. Rev.* **C97**(2), 024901 (2018).

[27] Cepila, J., Contreras, J. G., Krelina, M., and Tapia Takaki, J. D. *Nucl. Phys.* **B934**, 330–340 (2018).

[28] Andreev, V. et al. *Eur. Phys. J. C* **80**(12), 1189 (2020).

[29] Bendova, D., Cepila, J., and Contreras, J. G. *Phys. Rev.* **D99**(3), 034025 (2019).

[30] Bendova, D., Cepila, J., Contreras, J. G., and Matas, M. *Phys. Lett. B* **817**, 136306 (2021).

[31] Krelina, M., Goncalves, V. P., and Cepila, J. *Nucl. Phys.* **A989**, 187–200 (2019).

5 Publication list

1. Cepila, J.; Contreras, J. G.; Tapia Takaki, J. D., **Energy dependence of dissociative J/Ψ photoproduction as a signature of gluon saturation at the LHC**, Phys. Lett. B 766, pp. 186-191 (2017)
2. Cepila, J.; Contreras, J. G.; Krelina, M.,**Coherent and incoherent J/Ψ photonuclear production in an energy-dependent hot-spot model**, Phys.Rev. C97 (2018), 024901
3. Cepila, J.; Contreras, J. G.; Krelina, M.; Tapia Takaki, J. D., **Mass dependence of vector meson photoproduction off protons and nuclei within the energy - dependent hot-spot model**, Nucl.Phys. B934 (2018) 330-340
4. Bendova, D.; Cepila, J.; Contreras, J. G., **Dissociative production of vector mesons at electron-ion colliders** , Phys. Rev. D 99, 034025 (2019)
5. Cepila, J.; Contreras, J. G.; Matas, M., **Collinearly improved kernel suppresses Coulomb tails in the impact-parameter dependent Balitsky - Kovchegov evolution**, Phys.Rev. D99 (2019) 051502
6. Krelina M., Nemchik J., Pasechnik R., Cepila J., **Spin rotation effects in diffractive electroproduction of heavy quarkonia**, Eur.Phys.J. C79 (2019) no.2, 154
7. Cepila, J.; Nemchik, J.; Krelina, M.; Pasechnik, R., **Theoretical uncertainties in exclusive electroproduction of S-wave heavy quarkonia**, Eur.Phys.J. C79 (2019) no.6, 495
8. Krelina, M.; Goncalves, V. P.; Cepila, J., **Coherent and incoherent vector meson electroproduction in the future electron - ion colliders: the hot - spot predictions**, Nucl.Phys. A989 (2019) 187-200
9. Bendova, D.; Cepila, J.; Contreras, J. G.; Matas, M., **Solution to the Balitsky - Kovchegov equation with the collinearly improved kernel including impact - parameter dependence**, Phys.Rev. D100 (2019) no.5, 054015
10. Cepila, J.; Contreras, J. G.; Matas, M., **Predictions for nuclear structure functions from the impact - parameter dependent Balitsky - Kovchegov equation**, Phys. Rev. C 102, 044318
11. Bendova, D.;, Cepila, J.; Contreras, J. G. and Matas, M., **Photonuclear J/ψ production at the LHC: proton-based versus nuclear dipole scattering amplitudes**, ePrint arXiv:2006.12980 (2020) (to be published at Phys. Lett. B)
12. Cepila, J.; Matas, M., **Contribution of the nonlinear term in the Balitsky - Kovchegov equation to the nuclear structure functions**, Eur. Phys. J. A 56, 232 (2020)
13. Bendova, D.; Cepila, J.; Contreras, J. G.; Goncalves, V. P. and Matas, M., **Diffractive deep-inelastic scattering in future electron - ion colliders**, Eur.Phys.J.C 81 (2021) 3, 211

Curriculum vitae - Ing. Jan Čepila, Ph.D.

EDUCATION	**Ph.D.** - Nuclear Engineering specialization at FNSPE CTU in Prague **Ing.** - Experimental Nuclear Physics specialization at FNSPE CTU in Prague
WORK EXPERIENCE	Research assistant at the Department of Physics, FNSPE CTU in Prague Member of the European center for theoretical studies ECT*, Trento, Italy Member of the Management Committee of COST action CA15213 Member of the ALICE collaboration at LHC, CERN Member of the state exams committee of Experimental Nuclear and Particle Physics specialization at FNSPE CTU in Prague
ACTIONS ORGANIZATION	Member of local organizing committee of MPI@LHC 2019 workshop Member of local organizing committee of COST-THOR Spring School Chair of organizing committee od COST Indian-summer School 2018 Main organizer of annual EJČF Winter workshop
TEACHING EXPERIENCE	Department of Physics, FNSPE CTU in Prague Lectures of Subatomic Physics Creator of Specialized laboratories 1,2 Exercise in Basics of Quantum Chromodynamics Co-author of Accreditation file of Experimental Nuclear and Particle Physics specialization in 2012-2020 and Nuclear and Particle Physics specialization in 2020-2030
PUBLICATION ACTIVITIES	**Scientific publications:** 13 papers in peer-reviewed international journals 10 proceedings from international conferences co-author in the ALICE collaboration in 2015-2016 - approx. 68 papers H-index 7 106 citations (excluding auto-citations) **Propagation:** 2 popular articles in Pražská technika and Technicall journal Translation of info materials about ATLAS and ALICE experiments for CERN into Czech
STUDENTS SUPERVISION	Experimental Nuclear and Particle Physics specialization at FNSPE CTU in Prague 3 successfully defended diploma theses Nuclear Engineering specialization at FNSPE CTU in Prague 1 successfully defended PhD thesis as a co-supervisor 2 active PhD students currently
OTHER ACTIVITIES	Administrator of the library at the Department of Physics FNSPE CTU in Prague Main creator of web pages of FNSPE, of the Department of Physics at FNSPE, of the Nuclear and Particle Physics specialization IT administrator of the Department of Physics at FNSPE CTU in Prague Member of the admin team of computing cluster SUNRISE at the Department of Physics FNSPE CTU in Prague Webmaster of COST EU action Theory of hot matter and relativistic heavy-ion collisions